CHITOSAN-COATED CELLULOSE/SOY PROTEIN MEMBRANES WITH IMPROVED PHYSICAL PROPERTIES AND HEMOCOMPATIBILITY

Xiaomei Wang,[a] Peter R. Chang,[b] Zonghuan Li,[a] Hui Wang,[c] Hui Liang,[a] Xiaodong Cao,[d,*] and Yun Chen [a,*]

A series of cellulose/soy protein membranes (CSM) was coated with chitosan to improve the mechanical properties, cytocompatibility, and hemocompatibility. The original CSM and chitosan-coated CSM (CH/CSM) were characterized by Fourier transform infrared spectroscopy, X-ray diffraction analysis, scanning electron microscopy, water contact angle testing, and tensile testing. CH/CSM had a smoother surface microstructure and enhanced mechanical properties as compared to the corresponding CSM. The cytocompatibility and hemocompatibility of CSM and CH/CSM were evaluated by cell culture, MTT assay, in vitro platelet adhesion testing, plasma recalcification time (PRT) measurement, and hemolysis assay. The higher cell adherence and improved cytocompatibility of CH/CSM were mainly ascribed to the coated composition and the altered surface microstructure of CSM. CH/CSM also showed lower platelet adhesion, longer PRT, and a lower hemolysis rate, all resulting from the good hemocompatibility of chitosan and the smoother membrane surface after chitosan coating. Undoubtedly, surface coating with chitosan improved the microstructure, mechanical properties, cytocompatibility, and hemocompatibility, thus widening the possible range of applications for cellulose/soy protein-based biomaterials.

Keywords: Chitosan; Cellulose; Soy protein isolate; Coating; Mechanical properties; Hemocompatibility

*Contact information: a: Department of Biomedical Engineering, School of Basic Medical Science, Wuhan University, Wuhan 430071, China; b: Bioproducts and Bioprocesses National Science Program, Agriculture and Agri-Food Canada, 107 Science Place, Saskatoon, S7N 0X2, SK, Canada; c: Department of Pharmacology, School of Basic Medical Science, Wuhan University, Wuhan 430071, China; d: School of Materials Science and Engineering, South China University of Technology, Guangdong 510640, China; *Corresponding author: caoxd@scut.edu.cn, yunchen@whu.edu.cn*

INTRODUCTION

Cellulose, the most abundant natural polymer in the world, has been widely used in the fields of agriculture, construction, packaging, papermaking, feedstuff, drug additives, and biomaterials (Schurz 1999; Klemm et al. 2005; Entcheva et al. 2004; Luo and Zhang 2010; Cai et al. 2007). As biomaterials, cellulose and its derivatives have been fabricated into hemodialysis membranes (Abe and Mochizuki 2003), enzyme immobilization membranes (Bryjak et al. 2007), surgical haemostatic sponges (Sharma et al. 2007), and tissue engineering scaffolds (Müller et al. 2006) due to their biodegradeability, biocompatibility, and nontoxicity to cells and tissue. Soy protein isolate (SPI), one of the most commonly available plant proteins in the world, has been used in

nutritional foods (Eller and Reimer 2010), environmentally friendly adhesives (Qi and Sun 2010), and biodegradable plastics (Kumar et al. 2008), as well as in biomedical materials (Giavaresi et al. 2010). In the biomedical field, SPI has been used as a biodegradable matrix for drug delivery (Vaz et al. 2003), a serum-free medium for cell culture (Lee et al. 2008), and as scaffolds for tissue engineering (Merolli et al. 2010). In the *in vitro* cell culture environment, SPI is easily degraded, and the hydrolyzates from SPI promote cell growth (Franěk et al. 2000). To combine the virtues of both cellulose and SPI, in our previous works we had prepared a series of cellulose/SPI membranes and sponges (Chen and Zhang 2004; Chen et al. 2004; Luo et al. 2008, 2010). These cellulose/SPI composites exhibited good cytocompatibility with African green monkey kidney epithelial cells (Vero-E6) (Chen et al. 2004), human umbilical vein endothelial cells (ECV-304) (Luo et al. 2008), and mouse lung fibroblasts (L929) (Luo et al. 2010). However, the hemocompatibility of the cellulose/SPI composites needs to be further improved for application as biomaterials in direct contact with blood.

Chitosan is a partially deacetylated derivative of chitin. The physical, chemical, and mechanical properties of chitosan, along with its outstanding biocompatibility, biodegradability, bio-adhesiveness, nontoxicity, nonimmunogenicity, antibacterial action, and antifungal activity, make it an ideal material for use in a variety of biomedical and pharmaceutical applications, such as hemodialysis membranes, artificial skin, wound dressings, and drug delivery systems (Kumar 2000). Because of these unique properties, chitosan has been widely used, either alone as a biomaterial or to modify other biomaterials, for improved cytocompatibility and hemocompatibility (Cui et al. 2003; Xiao et al. 2008). For example, chitosan can be adsorbed on the surface of cellulose films because of the strong interactions between cellulose and chitosan molecules (Da Róz et al. 2010). It has also been reported that the incorporation of chitosan into SPI improved the biological properties of soy protein-based biomaterials (Silva et al. 2005). We hypothesized that chitosan could interact with both cellulose and SPI when chitosan was used to modify cellulose/SPI composites by blending or surface coating, and would improve biological properties of the resultant composites.

Coating is the simplest way to modify the surfaces of biomaterials for the improvement of surface characteristics (e.g. physical and biochemical properties) (Da Róz et al. 2010) and biological performance (e.g. cytocompatibility and hemocompatibility) (Shen et al. 2010), and for the installation of new functionalities to the original biomaterials (Uyama et al. 1998). Thus, in this study surface coating with chitosan was used to modify prepared cellulose/SPI membranes with the aim of enhancing physical properties, cytocompatibility, and hemocompatibility of the resultant composites. The surface characteristics and properties of the original and chitosan-coated cellulose/SPI membranes were comparatively investigated.

EXPERIMENTAL

Materials

Cotton linter (cellulose) was supplied by Hubei Chemical Fiber Group Co. Ltd. (Xiangfan, China). Its viscosity-average molecular weight (M_η) was measured by

viscosimetry in cadoxen to be 10.1×10^4 Daltons (Da). Commercial soy protein isolate (SPI) was supplied by DuPont Yunmeng Protein Technology Co. Ltd. (Yunmeng, China). Chitosan (MW 50000 Da, DD 91.2%) was purchased from Xingcheng Biological Products Factory (Nantong, China). Cotton linter, SPI, and chitosan were vacuum-dried for 24 h at 60 ºC before use. Other chemicals were analytical grade reagents used without further treatment.

Preparation of Cellulose/SPI Membranes

Cellulose/SPI membranes were prepared according to our previous method (Luo et al. 2008). Briefly, an aqueous 7% NaOH/12% urea solution was used as solvent for cellulose and SPI. The NaOH/urea solution was pre-cooled to -12.5 ºC before a designated amount of dry cellulose was immersed in the solvent and stirred for about 5 min at ambient temperature to give a transparent cellulose solution (Cai et al. 2008). The concentration of cellulose was 3.5 wt%. SPI was dispersed in the above NaOH/urea solvent at room temperature to obtain slurry with a SPI content of 10 wt%. The SPI slurry was mixed with the cellulose solution to obtain solutions with SPI contents of 10, 30, or 50 wt% (W_{SPI}, weight of SPI based on the total mass of dry cellulose and SPI). The mixture was stirred at room temperature for 30 min and degassed at 10 ºC by centrifuging for 10 min at 7,500 × g. It was then cast on a glass plate to make a gel sheet with a thickness of about 200 μm. The gel sheets were soaked in 5 wt% acetic acid aqueous solution for 5 min, and transparent membranes were obtained after the occurrence of apparent coagulation. Subsequently, membranes were washed with water and coded as CSM-*n*, where CSM meant cellulose/soy protein isolate membrane, and *n* corresponded to the initially designated SPI content. For example, CSM-10 corresponded to the cellulose/SPI membrane containing 10 wt% SPI. When *n* was 0, the membrane was pure cellulose with no addition of SPI.

Surface Coating of CSM-*n* Membranes with Chitosan

Surface coating was carried out according to a similar method, as reported in previous work (Lü et al. 2009). Chitosan was dissolved in a 2% acetic acid aqueous solution. The dry CSM-*n* cellulose/SPI membranes, which were around 0.06 mm thick, were coated with 1 wt% chitosan solution and then heated at 40 ºC for 8 h. The membranes were dipped into ammonia solution for a few seconds to neutralize the acetic acid, washed with distilled water for 30 min, and then air-dried at room temperature. The resulting chitosan-coated membranes were coded as CH/CSM-*n* (*n* = 0, 10, 30, 50). Chitosan membrane was prepared by the same method mentioned above and was coded as CM.

Characterization of Structure and Physical Properties

Fourier transform infrared (FTIR) spectroscopy

CSM-*n* and CH/CSM-*n* membranes were vacuum-dried at 60 ºC for 24 h, and then ground into powders before they were pelletized with KBr for FTIR measurements. FTIR spectra were recorded on an FTIR spectrometer (Model 1600, Perkin-Elmer Co., USA) over a wavenumber range of 4000 to 400 cm^{-1}.

X-ray diffraction analysis

The CSM-*n* and CH/CSM-*n* membranes were vacuum-dried at 60 ^{o}C for 24 h. The X-ray diffraction (XRD) patterns of the original materials and resulting membranes were recorded on a D8 Advance X-ray Diffraction instrument (Bruker AXS, Germany), using Cu K_α radiation (λ = 0.154 nm) at 40 kV and 30 mA with a scan rate of 4^{o} min^{-1}. The diffraction angle ranged from 4 to 40^{o}.

Morphology of the membranes

The morphology of CSM-*n* and CH/CSM-*n* membranes was observed on a scanning electron microscope (SEM, S-570, Hitachi, Japan) with an accelerating voltage of 20 kV. The wet membranes were frozen in liquid nitrogen, fractured immediately, and vacuum-dried. The surfaces and cross-sections of the membranes were coated with gold for SEM observation.

Water contact angle measurement

The static water contact angle was measured to monitor the change in wettability of CM, CSM-*n* and CH/CSM-*n* surfaces before and after coating. Briefly, a 2 μL drop of distilled water was placed on the membrane surface and the static contact angle was measured using a goniometer (First Ten Angstroms, Inc., Portsmouth, VA, USA) at 25 ºC with 60 % relative humidity. For each reported contact angle value, three measurements were obtained from different areas of the surface, and the average was taken.

Tensile testing

The mechanical properties of membranes equilibrated at 46% relative humidity for 1 week and of membranes soaked in water for 1 h were respectively tested on a universal testing machine (CMT6503, Shenzhen SANS Test Machine Co. Ltd., China) according to ISO6239-1986 (*E*) at a tensile rate of 10 mm/min. The mean values of the tensile strength (σ_b), the elongation at break (ε_b), and the standard deviations for the membranes in dry and wet states were obtained from measurements on four pieces of specimen. Water resistivity (R_σ) of the membranes was evaluated from the tensile strength of the membranes equilibrated at 46% relative humidity for 1 week (σ_b) and of the membranes soaked in water for 1 h ($\sigma_{b,\,wet}$) by the following equation:

$$R_\sigma = 100 \times (\sigma_{b,\,water} / \sigma_b) \quad (1)$$

In Vitro Evaluation of Cytotoxicity and Cytocompatibility

Cell culture

A cell line of mouse lung fibroblasts (L929, provided by China Center for Type Culture Collection, Wuhan University) was used in this work. L929 cells were routinely grown and maintained in Dulbecco's Modified Eagle's Medium (DMEM, Gibco Life) containing 10% (v/v) fetal bovine serum (FBS, Gibco Life), 100 IU/mL penicillin, and 100 μg/mL streptomycin. After 70 to 80% confluence, the cells were digested with 0.25% trypsin and passaged. The cell density was adjusted to 1×10^7 cells/mL.

In vitro cytotoxicity of the membranes was evaluated by the extract test and the direct contact test according to the ISO standard (ISO 10993-5 1999).

Extract test: Samples were extracted in culture medium at 37 ºC for 24 h. The 3-(4,5-dimethylthiazol-2-yl)-2,5-diphenyltetrazolium bromide (MTT) assay was used to measure the relative cell viability. The extracts were placed in contact with a monolayer of L929 cells in 96-well tissue plates. Cells cultured in the culture medium were used as a control. After incubating for 1, 3, 5, and 7 days, 20 μL of MTT solution (5 mg/mL, Sigma) was added into each well, followed by 4 h of incubation at 37 ºC. After removal of the culture medium, formazan crystals were dissolved by adding 150 μL of DMSO at 37 ºC for 15 min (Silva et al. 2005). The absorbance of the solution was measured via a spectrophotometer at 570 nm using a microplate reader (GENios, Tecan, Austria).

Direct contact test (Serrano et al. 2004): Selected CSM-*n* and CH/CSM-*n* membranes were cut into 2 × 2 cm^2 pieces and sterilized by UV-radiation with a wavenumber of 254 nm for 30 min. The sterilized membranes were transferred into 24-well tissue culture polystyrene plates (TCPS, Costar), and blank culture plates were used as negative controls. L929 cells were seeded onto each membrane or control plate with a density of 1 × 10^5 cells/well. The culture plates were incubated at 37 °C in 5% CO_2 humidified atmosphere. After 48 h, the cells cultured on the membranes, and controls were fixed in 2.5 wt% glutaraldehyde, then progressively dehydrated in ethanol, dried in super-critical CO_2, and finally coated with gold for observation of cell morphology and density using SEM (S-570, Hitachi, Japan) with 20 kV accelerating voltage (Serrano et al. 2004). Cell densities of the cells attached to the surfaces of the membranes were calculated from the SEM photographs in a selected area (480 μm × 480 μm corresponding to the area in the original membrane) using a high-resolution imaging treatment system (HLPAS-1000, Tongji Medical College, Huazhong University of Science and Technology, Wuhan, China). The cell density and standard deviation were calculated from three independent SEM photographs of each sample (Suzuki et al. 2005).

Anticoagulation Properties

Preparation of blood and plasma (Shen et al. 2010)

Blood was drawn from healthy New Zealand rabbits, and then mixed with 3.8 wt% citrate acid solution (blood: citrate acid = 9: 1). Fresh whole blood was centrifuged at 1000 rpm (revolutions per minute) for 10 min or at 3000 rpm for 20 min at room temperature to obtain platelet-rich plasma (PRP) and platelet-poor plasma (PPP), respectively.

Platelet adhesion testing (Zhao et al. 2010)

The CSM-*n* and CH/CSM-*n* membranes (1 cm × 1 cm) were soaked in 100 μL of fresh PRP in a 24-well plate at 37 °C for 30 min. After incubation, the samples were gently rinsed with PBS to remove loosely adhering platelets from the surface. The samples were fixed in 2.5% glutaraldehyde for 4 h at room temperature, washed with PBS, and dehydrated in a series of increasing ethanol concentrations. They were then dried in super-critical CO_2 and coated with gold. The morphology of adherent platelets was observed by SEM. The number of platelets adhered to the membranes was investigated via photographs using computer-aided image analysis software (Image-Pro-Plus, Media Cybernetics, USA). Five randomly selected SEM images were used to calculate the number of platelets adhered to the membranes (Roy et al. 2009).

Plasma recalcification time (PRT) (Shen et al. 2010)

The CSM-*n* and CH/CSM-*n* membranes (1 cm × 1 cm) were soaked in 200 μL of fresh PPP at 37 °C for 10 min. Then, 100 μL calcium chloride solution (0.025 mol/L) was immediately added to the PPP. The mixture was observed until silky fibrin started to appear. The time interval between the addition of the solution and the appearance of silky fibrin was recorded as PRT. TCPS was used as a control. The test was repeated four times for each sample.

Hemolysis test (Shen et al. 2010)

The CSM-*n* and CH/CSM-*n* membranes were cut into 1 cm × 1 cm pieces. Every piece of membrane was put into a tube and rinsed with distilled water and normal saline three times. Saline solution (10 mL) was then poured into the tube, and it was placed in a shaking bath for 30 min at 37 °C. A quantity of 0.2 mL diluted rabbit whole blood (8 mL whole blood was diluted by 10 mL normal saline) was then added to the tube, and the membrane allowed to soak in the blood/saline solution for 60 min at 37 °C. Distilled water and normal saline were used as positive and negative controls, respectively, and were treated in the same way as above. The tubes were centrifuged at 1500 rpm for 10 min, after which the absorbency of the clear upper solution was measured with a spectrophotometer (Lambda 25, PerkinElmer, USA) at 545 nm. Three parallel experiments were performed for each sample. The hemolysis rate (*HR*) was calculated as follows,

$$HR = (AS - AN) / (AP - AN) \quad (2)$$

where *AS*, *AP*, and *AN* were the absorbencies of the experimental sample, the positive control, and the negative control, respectively.

RESULTS AND DISCUSSION

Structure and Physical Properties

FTIR analysis

The FTIR spectra of CSM-*n*, CH/CSM-*n*, chitosan powder, and SPI powder are given in Fig. 1A and 1B. The CSM-0 showed an FTIR spectrum typical of cellulose. In the FTIR spectra of CSM-10 and CSM-30 membranes, a new absorption peak occurred at around 1539 cm^{-1} (amide II) due to the incorporation of SPI into cellulose (Luo et al. 2008). After the CSM-*n* was surface coated with chitosan, the spectra of the CH/CSM-*n* exhibited a few minor changes compared with the CSM-*n*. Because SPI and chitosan contain the same amide and amino groups, most of the SPI absorption peaks overlapped with those of chitosan in CH/CSM-*n* (*n* = 10, 30, and 50) such as the peaks around 3400 to 3450 cm^{-1}, 1635 cm^{-1}, and 1320 cm^{-1}. It was difficult to find these changes simply by comparing the FTIR spectra of the CSM-10, CSM-30, and CSM-50 with those of the corresponding CH/CSM-10, CH/CSM-30, and CH/CSM-50. Because there was no SPI in the neat cellulose membrane (CSM-0), the differences in the spectra of CSM-0 and that of CH/CSM-0 could be identified from the high magnification spectra of CSM-0,

CH/CSM-0, and chitosan powders shown in Fig. 1B. The FTIR spectrum of chitosan powder displays bands at 3400-3450 cm^{-1} (-OH and -NH groups stretching vibrations), 2874-2922 cm^{-1} (C-H stretching), 1650 cm^{-1} (C=O, amide I), 1599 cm^{-1} (-NH_2 groups), 1560 cm^{-1} (-NH- groups), 1380 cm^{-1} (CH_3 deformation), 1309 cm^{-1} (C-N stretching, amide III), 1079 cm^{-1} (amine C-N stretching vibration), and 1150-1085 cm^{-1} (ether bonding) (Almeida et al. 2010). Compared with the FTIR spectrum of CSM-0, it was observed that new peaks occurred at 1650, 1599, 1560, and 1421 cm^{-1} in the CH/CSM-0 spectrum, which were from C=O (amide I), -NH_2, -NH-, and -COO^- (symmetric stretching) groups of chitosan, respectively (Almeida et al. 2010; Pawlak and Mucha 2003). This indicated that the chitosan-coating of CSM-0 was successful.

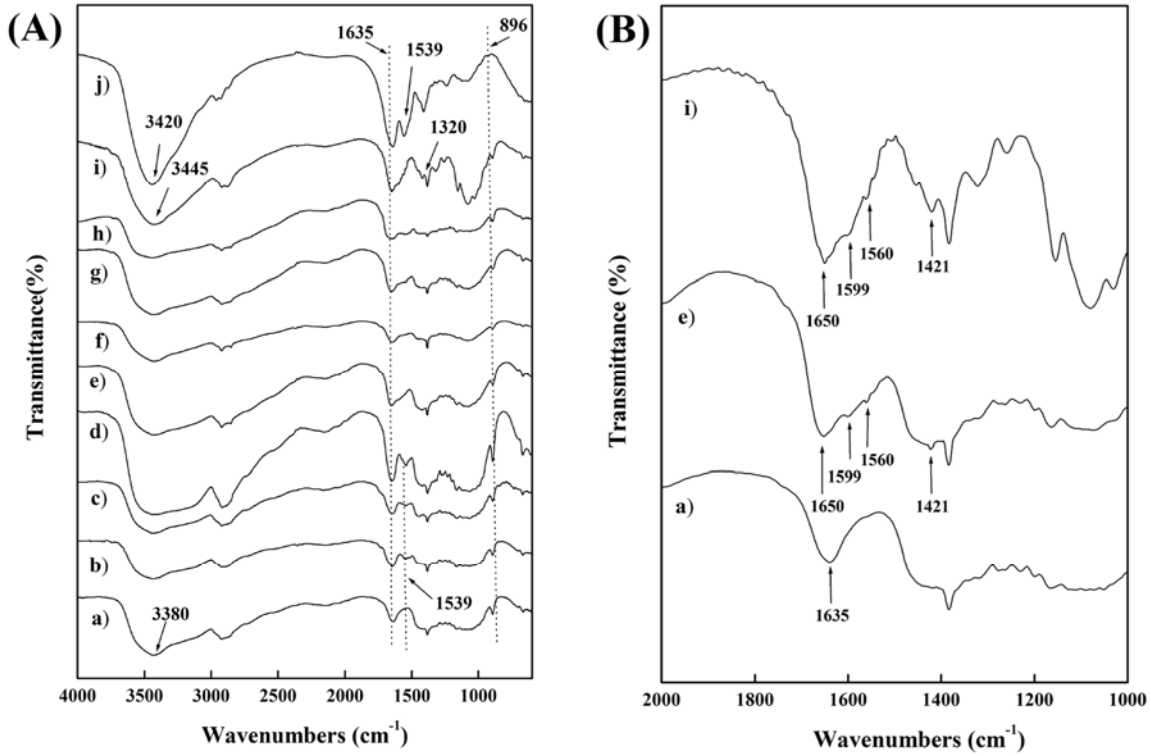

Fig. 1. FTIR spectra of CSM-n and CH/CSM-n (n = 0, 10, 30, and 50): (a) CSM-0; (b) CSM-10; (c) CSM-30; (d) CSM-50; (e) CH/CSM-0; (f) CH/CSM-10; (g) CH/CSM-30; (h) CH/CSM-50; (i) chitosan powder; (j) SPI powder

XRD analysis

The XRD patterns of CSM-*n* and CH/CSM-*n* (*n* = 0, 10, 30, and 50) membranes are shown in Fig. 2. No obvious differences were observed in the shape and position of the peaks between the XRD pattern of CSM-*n* and CH/CSM-*n* membranes. However, the relative intensity of the diffraction peaks in the XRD pattern of CH/CSM-*n* was higher than that of the corresponding CSM-*n*. This may be attributed to the chitosan coated on the surface of the cellulose/SPI membranes.

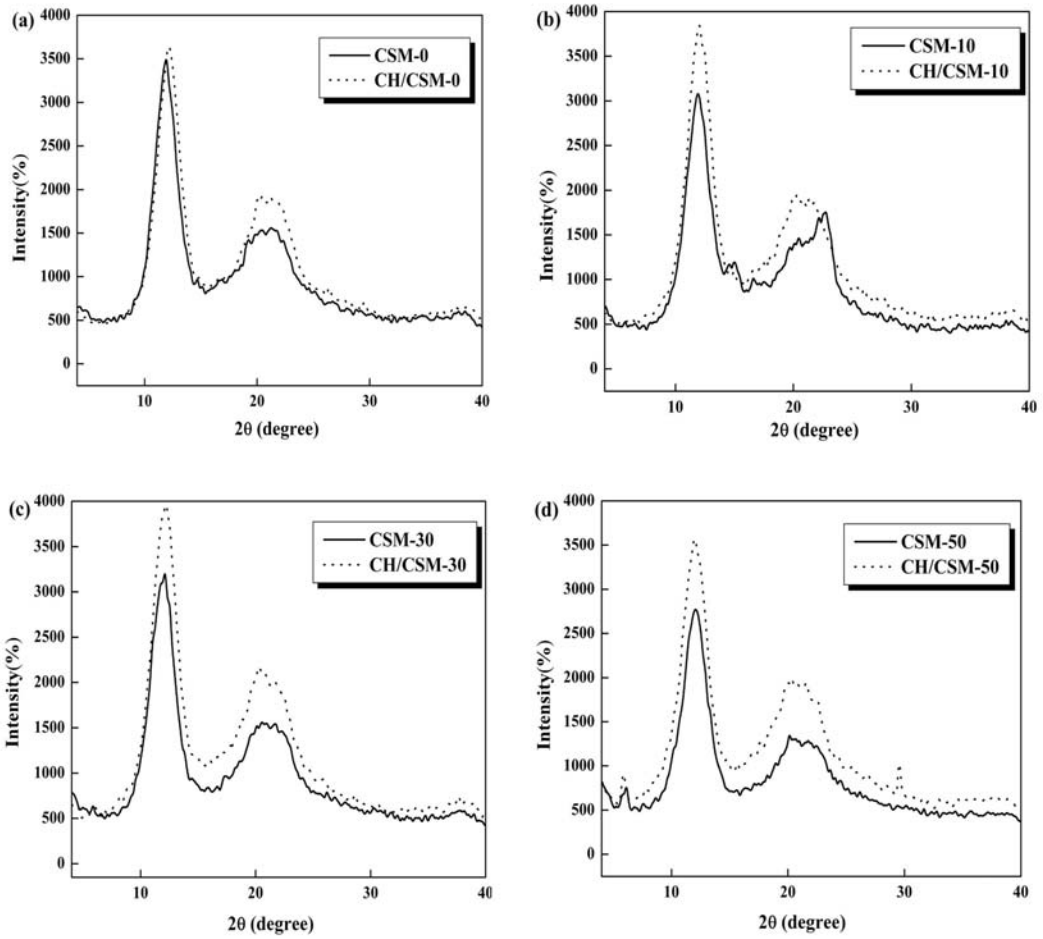

Fig. 2. XRD patterns of CSM-*n* and CH/CSM-*n* (*n* = 0, 10, 30, and 50)

SEM analysis

SEM photographs of the surfaces of CSM-*n* and CH/CSM-*n* are shown in Fig. 3. The original CSM-*n* had a rough and porous structure, and the pore size increased as the SPI content increased. This is consistent with the findings of our previous work (Luo et al. 2008). After coating with chitosan, the pores on the surface of the original membranes almost disappeared, and the surfaces of the CH/CSM-*n* became smoother than those of the corresponding CSM-*n*. This may be due to chitosan entering into the pores or covering the pores on the CSM-*n* by forming a very thin layer during the coating process. The differences between the SEM images of CSM-*n* and CH/CSM-*n* indicated that chitosan had successfully coated and adhered to the surface of CSM-*n*, and that the chitosan-coating had altered the surface morphology of the original CSM-*n*. These changes may affect the microstructure, physical properties, and biological properties of the resulting membranes.

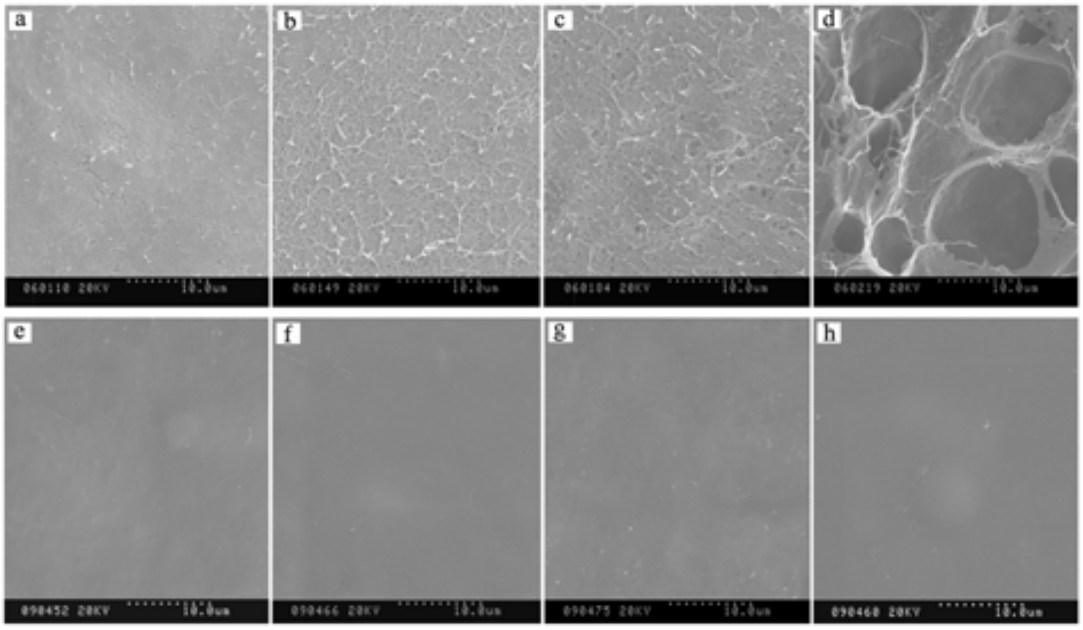

Fig. 3. SEM photographs of the surfaces of CSM-*n* and CH/CSM-*n* (*n* = 0, 10, 30, and 50): (a) CSM-0; (b) CSM-10; (c) CSM-30; (d) CSM-50; (e) CH/CSM-0; (f) CH/CSM-10; (g) CH/CSM-30; (h) CH/CSM-50

Water contact angle measurement

Contact angle measurement provides a simple and convenient way to evaluate the hydrophilicity and/or hydrophobicity of a material's surface (Qu et al. 2006). Fig. 4 shows the water contact angles on the surfaces of CM, CSM-*n* and CH/CSM-*n*.

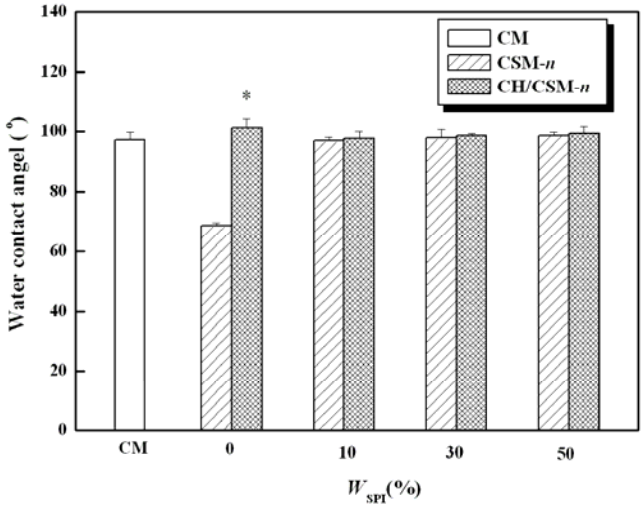

Fig. 4. Water contact angle of chitosan membrane (CM), CSM-*n* and CH/CSM-*n* (*n* = 0, 10, 30, and 50) *P < 0.05 (CSM-*n* compared to CH/CSM-*n*)

The water contact angles of CSM-10, CSM-30, and CSM-50 were very similar and were obviously higher than that of the neat cellulose membrane (CSM-0) because of the relatively higher hydrophobicity of globulin protein molecules compared with cellulose. After surface coating with chitosan, the water contact angle of CH/CSM-0 was higher than that of the original CSM-0 membrane ($P < 0.05$), because chitosan is more hydrophobic than cellulose. As shown in Fig. 4, the water contact angle of neat chitosan membrane (CM) was higher than that of neat cellulose membrane (CSM-0). The values of the water contact angles for the CH/CSM-10, CH/CSM-30, and CH/CSM-50 were, however, very close to those of the corresponding original membranes. This indicated that chitosan and SPI had very close hydrophilicity/hydrophobicity, so the chitosan coating did not obviously change the surface hydrophilicity of the CSM-10, CSM-30, and CSM-50.

Mechanical properties of the membranes

The tensile strength and elongation at break (σ_b and ε_b, respectively) of CSM-*n* and CH/CSM-*n*, both equilibrated for 1 week at 46% relative humidity, are shown in Fig. 5a. The tensile strength and elongation at break of the membranes soaked for 1 h in water ($\sigma_{b,\ water}$ and $\varepsilon_{b,\ water}$) are shown in Fig. 5b. As shown in Fig. 5a, both the σ_b and ε_b values of the CSM-*n* and CH/CSM-*n* membranes first increased, reaching a maximum when W_{SPI} was 10 wt%, and then decreased gradually. When the SPI content was 10 wt%, it dispersed homogenously in the cellulose, forming strong interactions during the cellulose/SPI membrane fabrication process (Luo et al. 2008) resulting in maximized σ_b and ε_b values. It was confirmed in our previous work that phase separation between SPI and cellulose occurred when W_{SPI} was higher than 40% (Chen and Zhang 2004), resulting in decreased mechanical properties of the cellulose/SPI membranes.

Mechanical properties in the wet state are particularly important for biomaterials used for *in vitro* cell culture or *in vivo* implantation. As shown in Fig. 5b, the tensile strength of membranes soaked in water for 1 h ($\sigma_{b,\ water}$) was lower than that of the corresponding membranes that were not soaked in water (σ_b); however, elongation of the membranes soaked in water ($\varepsilon_{b,\ water}$) was higher than that of the unsoaked membranes. The increase in elongation for the water-soaked membranes was due to the plasticization effect of water on cellulose and SPI. After surface coating with chitosan, CH/CSM-*n* showed the same trend for changes in mechanical properties as the original CSM-*n*.

It was worth noting that the σ_b, ε_b, $\sigma_{b,\ water}$ and $\varepsilon_{b,\ water}$ values of all the CH/CSM-*n* were higher than those of the corresponding CSM-*n*, which meant that surface coating of chitosan enhanced the mechanical properties of CSM, with or without water-soaking of the membranes. As reported in previous work (Almeida et al. 2010; Da Róz et al. 2010), when chitosan was blended with cellulose or absorbed on the surface of cellulose it interacted with cellulose to form hydrogen bonding between the –OH and $–NH_2$ groups in chitosan and the –OH groups in cellulose. It was also reported that, due to their opposite charges, cationic chitosan interacted with anionic SPI to form a polyelectrolyte complex (Murakami and Takashima 2003) and to form strong hydrogen bonding (Silva et al. 2005). Therefore, chitosan could interact with cellulose and SPI together in the cellulose/SPI membranes where cellulose and SPI co-exist. In other words, the improvement of the mechanical properties was due to interactions between the chitosan

and SPI molecules, and between the chitosan and cellulose on the surface of CH/CSM. Furthermore, chitosan covered or filled the micropores of the original CSM-*n* to form a continuous smooth layer (as observed by SEM), which was more beneficial than the original porous microstructure for improving the tensile strength and flexibility of the membranes.

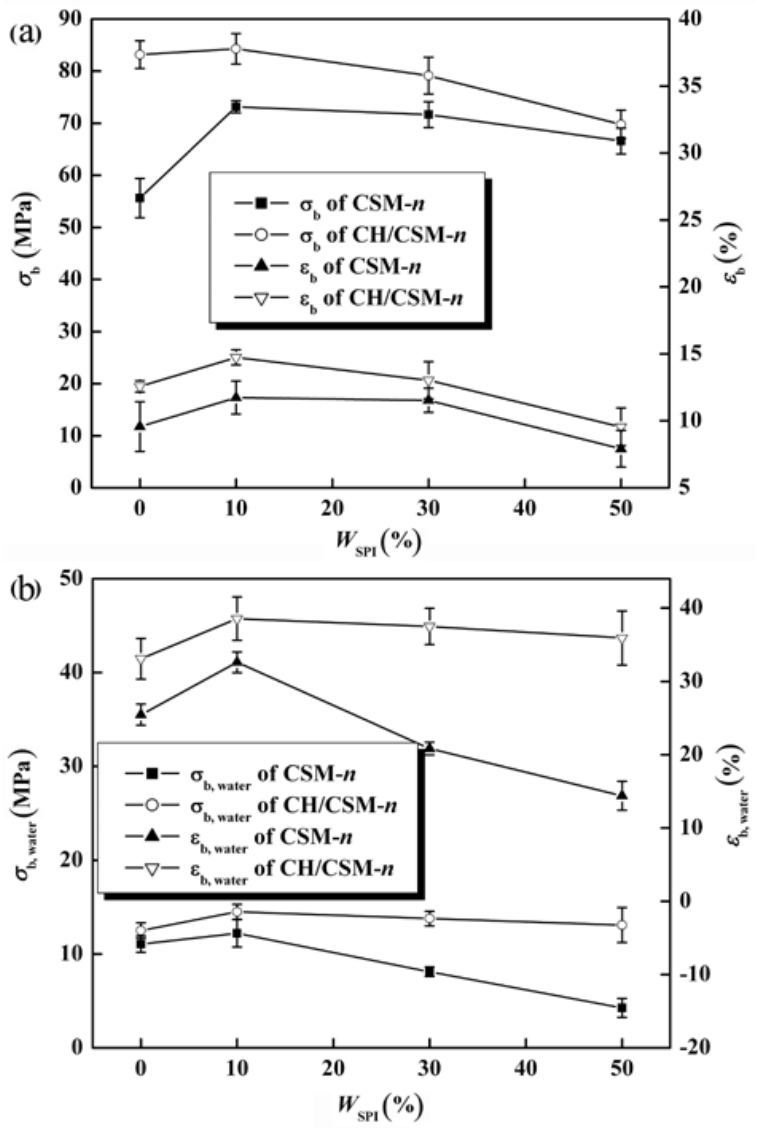

Fig. 5. Tensile strength and elongation at break of CSM-*n* and CH/CSM-*n* (*n* = 0, 10, 30, and 50) equilibrated at 46% relative humidity for 1 week (a) and those soaked in water for 1 h (b)

Results for the water resistivity (R_σ) are listed in Table 1. The R_σ of CSM-0, CSM-10, CSM-30, and CSM-50 were 19.88, 16.69, 11.33, and 6.40, respectively. After chitosan coating, the R_σ of CH/CSM-0, CH/CSM-10, CH/CSM-30, and CH/CSM-50 became 15.03, 17.21, 17.41, and 18.74, respectively. This showed that, except for the cellulose membrane (CSM-0), the water resistivity of the other CSM membranes

increased after chitosan coating. Interestingly, the higher the SPI content in the original membrane, the more the water resistivity increased. This may be due to the rich amino groups in SPI that result in strong hydrogen bond interactions between the molecular chains of chitosan and SPI, which increase the water resistivity and slow the dissolution of SPI from cellulose/SPI membranes into water.

Table 1. Comparison of Water Resistivity (R_σ) for CSM-*n* and CH/CSM-*n*

n	R_σ of CSM-*n*	R_σ of CH/CSM-*n*
0	19.88	15.03
10	16.69	17.20
30	11.33	17.41
50	6.40	18.74

R_σ of CSM-*n* = 100 × ($\sigma_{b,\ water}$ of CSM-*n* / σ_b of CSM-*n*)
R_σ of CH/CSM-*n* = 100 × ($\sigma_{b,\ water}$ of CH/CSM-*n* / σ_b of CH/CSM-*n*)

Cytocompatibility Evaluations

Cell viability

The MTT assay is based on mitochondrial viability, meaning that only functioning mitochondria can oxidize MTT to give the typical blue-violet end product (Lin et al. 2009). This assay is an indirect method for measuring cell viability and proliferation by correlating the optical density (OD) at 570 nm to cell numbers. Figure 5 shows the results of quantitative MTT testing for L929 fibroblast cultured in the extracts of CSM-*n* and CH/CSM-*n* membranes for 1, 3, 5, and 7 days. On the first day, the OD value in all the experimental groups was close to that of the control group, indicating low- or non-toxicity of the extracts at the beginning of cell culture. The OD value increased as cell culture time increased. The cells proliferated faster in CSM-10, CSM-30, and CSM-50 than in CSM-0 because the hydrolytes of SPI were beneficial for cell proliferation and growth (Lee et al. 2008). On the first and third day, there were no obvious differences between CSM-*n* and CH/CSM-*n*. On the fifth and seventh day, cell proliferation in the CH/CSM-*n* extracts was relatively higher than that of the corresponding CSM-*n* extracts. This indicated that the extracts from CSM-*n* and CH/CSM-*n* had no toxicity to the L929 cells over seven days, and in this case promoted cell proliferation.

Morphology and number of cells cultured on membranes

Cellular behavior on biomaterials is an important factor for evaluating their biocompatibility; and cell attachment and spreading are crucial for cell growth and differentiation (Cai et al. 2002). It was observed in Fig. 7 that the L929 cells grew well on the surfaces of the membranes, and that the morphology of cells on the CSM-*n* or CH/CSM-*n* membranes was very close to that of the control (glass plate). Most of the cells were shuttle-shaped and expanded very well on the membrane surfaces.

The cell density on the membranes is shown in Fig. 8. The average cell densities on the CSM-0, CSM-10, CSM-30, and CSM-50 were 2204, 2857, 2623, and 2453 cell/mm^2, respectively. These results showed that cell density depended on SPI content in the membranes. In fact, SPI content of a certain level was beneficial for the cells to adhere and grow on the membranes because the SPI incorporated in cellulose was gradually hydrolyzed in the cell culture medium and provided some nutrition for the cells (Lee et al. 2008; Luo et al. 2008). Over-incorporation of SPI (30 and 50 wt% SPI) may produce too high of a hydrolyte concentration in the cell-culture medium, resulting in a lower cell density on the surfaces of the membranes.

After surface coating with chitosan, the cell densities on CH/CSM-0, CH/CSM-10, CH/CSM-30, and CH/CSM-50 were 2822, 3266, 3206, and 2947, respectively, which was higher than on the corresponding CSM-*n* membranes. This indicated that the chitosan coating increased cell proliferation because chitosan itself was beneficial for cell growth (Cai et al. 2002; Xiao et al. 2008), and because the chitosan coating on the cellulose/SPI membranes retarded and prolonged the release of SPI from the membranes, which also promoted the cell growth.

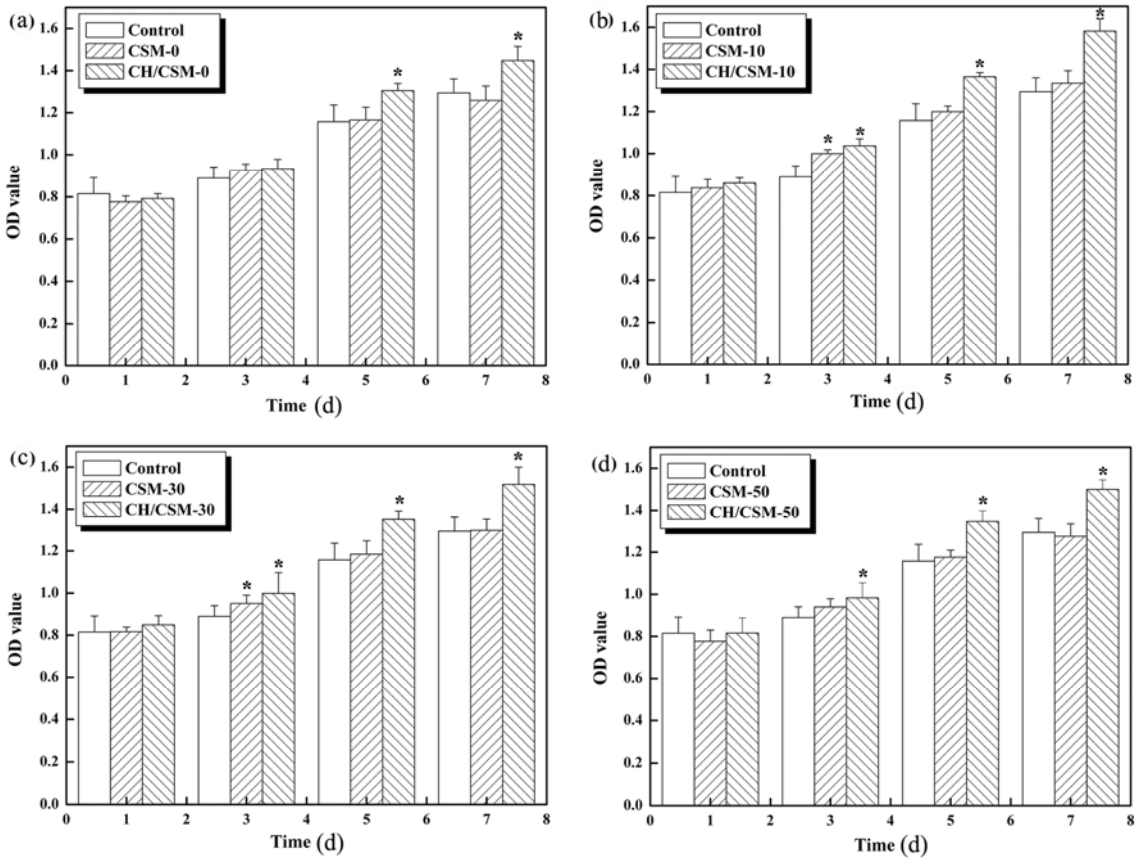

Fig. 6. Cell viability of L929 cultured in extracts from CSM-*n* and CH/CSM-*n* (*n* = 0, 10, 30, and 50) for 1, 3, 5 and 7 days, measured by MTT assay. *P < 0.05 (compared to the control on the same day)

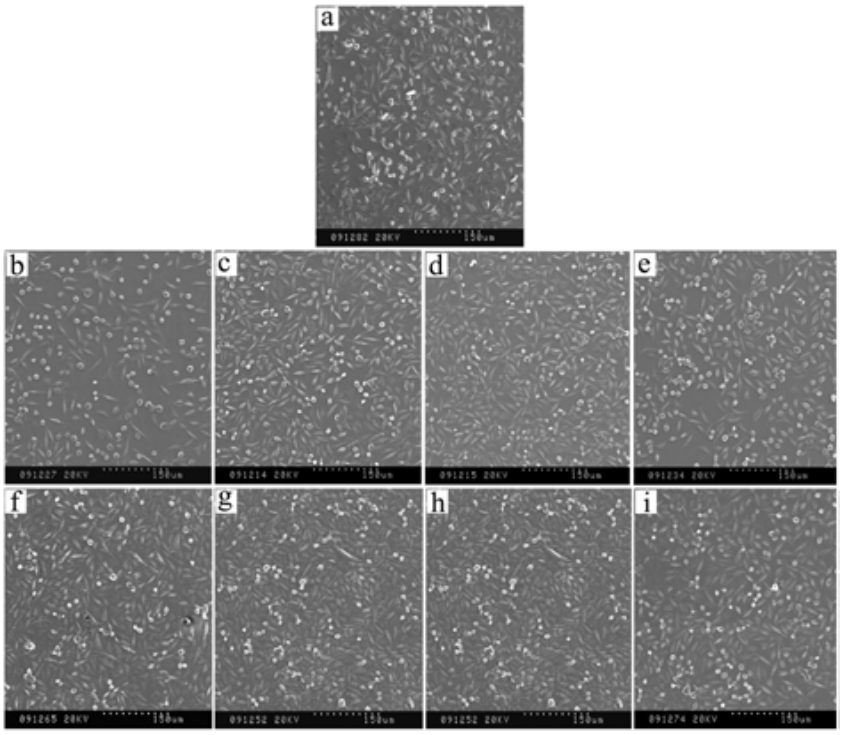

Fig. 7. SEM photographs of L929 cultured on the surface of CSM-*n* and CH/CSM-*n* (*n* = 0, 10, 30, and 50): (a) Control; (b) CSM-0; (c) CSM-10; (d) CSM-30; (e) CSM-50; (f) CH/CSM-0; (g) CH/CSM-10; (h) CH/CSM-30; (i) CH/CSM-50

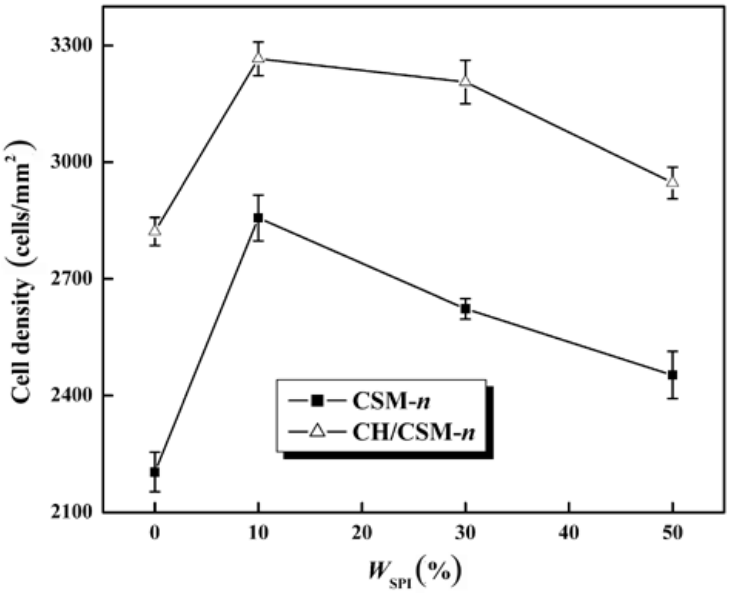

Fig. 8. Cell density of L929 attached to the surface of CSM-*n* and CH/CSM-*n* (*n* = 0, 10, 30, and 50)

Hemocompatibility Evaluation

Platelet adhesion

Platelet adhesion and activation on the surface of a biomaterial is the most essential characteristic in evaluating the hemocompatibility of a biomaterial (Guo et al. 2009; Roy et al. 2009). When blood contacts a foreign material, plasma proteins are adsorbed onto the material surface and provoke the adhesion of platelets, white blood cells, and some red blood cells onto the plasma protein layer. Adherent and aggregated platelets release materials such as adenosine diphosphate (ADP) and adenosine triphosphate (ATP), thereby inducing more platelet aggregation on the surface. In the final phase, a non-soluble fibrin network or thrombus is formed (Kang et al. 1996). SEM photographs of the adherent platelets on the surfaces of CSM-*n* and CH/CSM-*n* are shown in Fig. 9.

The number of adherent platelets on the membranes measured from SEM photographs is shown in Fig. 10. Platelets and platelet aggregates were observed on the original CSM-*n* surfaces, and the adherent platelets extended long pseudopodia spreading over the membrane surface. Platelets adhered sparsely to the CH/CSM-*n* surfaces, and the numbers of adhered platelets were obviously lower than on the corresponding CSM-*n*. Low platelet adhesion and activation denotes good hemocompatibility, while a higher degree of platelet adhesion and activation should result in the formation of a thrombus (Lin et al. 2009; Roy et al. 2009). Platelet adhesion testing in this work revealed that surface coating with chitosan decreased platelet adhesion and increased the hemocompatibility of the cellulose/SPI membranes. Interactions between membranes and platelets depended on the morphology and hydrophilicity of the membrane surfaces. The original CSM-*n* membranes absorbed many more platelets because of their rough surfaces, as shown in Fig. 9, which more easily provoked the adhesion of platelets, white blood cells, and some red blood cells onto the material. After coating with chitosan, the surfaces of the membranes became smooth. The hydrophilicity was not obviously changed, except for CH/CSM-0, and as a result, CH/CSM-*n* exhibited an anticoagulant property. This offers the possibility of its use in biomaterial devices in direct contact with blood.

Plasma recalcification time (PRT)

The intrinsic pathway of coagulation is triggered by surface contact, and uses a linear cascade of reactions requiring Ca^{2+} when viewed from the perspective of blood-biomaterial interactions. PRT serves as an important parameter of the intrinsic coagulation system (Liu et al. 2008).

Figure 11 shows the PRT values of CSM-*n* and CH/CSM-*n*. The average PRT value of CSM-0 was very close to the control (TCPS), while the PRT value of CSM-*n* increased with an increase in SPI content. The average PRT values of the CH/CSM-*n* (184 s ~ 239 s) were much higher than those of the control and the corresponding CSM-*n* (103 s ~ 183 s) were. There was a significant difference between the PRT values of CH/CSM-*n* and CSM-*n* ($p < 0.05$), indicating that surface coating with chitosan delayed plasma recalcification on the membrane surface resulting from the smoother surface and the anticoagulant effect of chitosan itself.

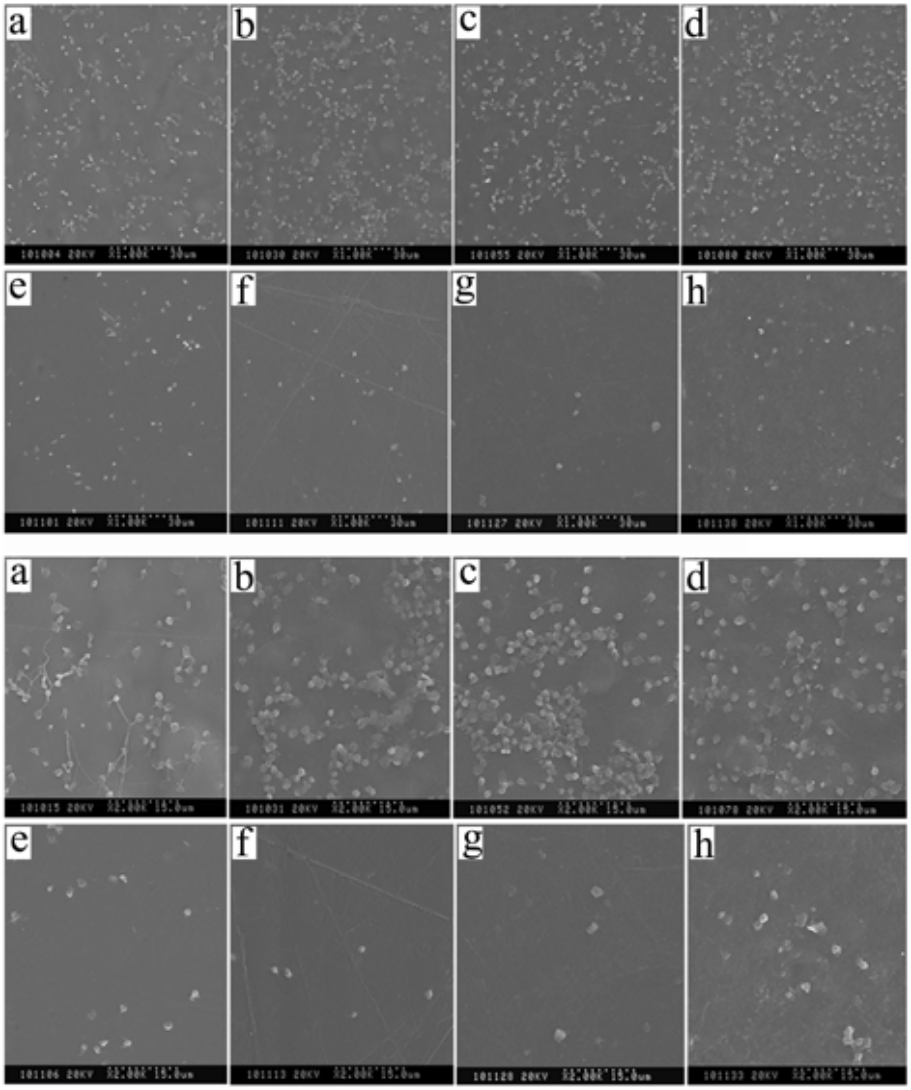

Fig. 9. Platelets adhered to CSM-*n* and CH/CSM-*n* (*n* = 0, 10, 30, and 50) with different magnification: (a) CSM-0; (b) CSM-10; (c) CSM-30; (d) CSM-50; (e) CH/CSM-0; (f) CH/CSM-10; (g) CH/CSM-30; (h) CH/CSM-50

Hemolysis Test

Hemolysis of blood is another problem associated with the biocompatibility of a material (Wen et al. 2010). *In vitro* hemolysis testing has been used as a simple and reliable way to estimate the blood compatibility of biomaterials (Zhang et al. 2009). The hemolysis rates (*HR*) of the negative and positive controls and of membranes, as calculated from the hemolysis tests, are summarized in Table 2. *HR* is regarded as safe when it is less than 5% (ISO 10993-4 1999). Wang et al. (2007) evaluated the *HR* of chitosan membranes and considered the membranes to be a safe carrier. The *HRs* of CSM-0 and CSM-10 were 1.56% and 1.57%, respectively, while those of CSM-30 and CSM-50 were higher than 5%. This suggested that SPI content in the original cellulose/SPI membranes exceeding 30% would result in an increased incidence of

hemolysis. The *HR* values of CH/CSM-*n* were all much lower than 5%, indicating that coating with chitosan indeed improved the hemocompatibility of the CSM membranes.

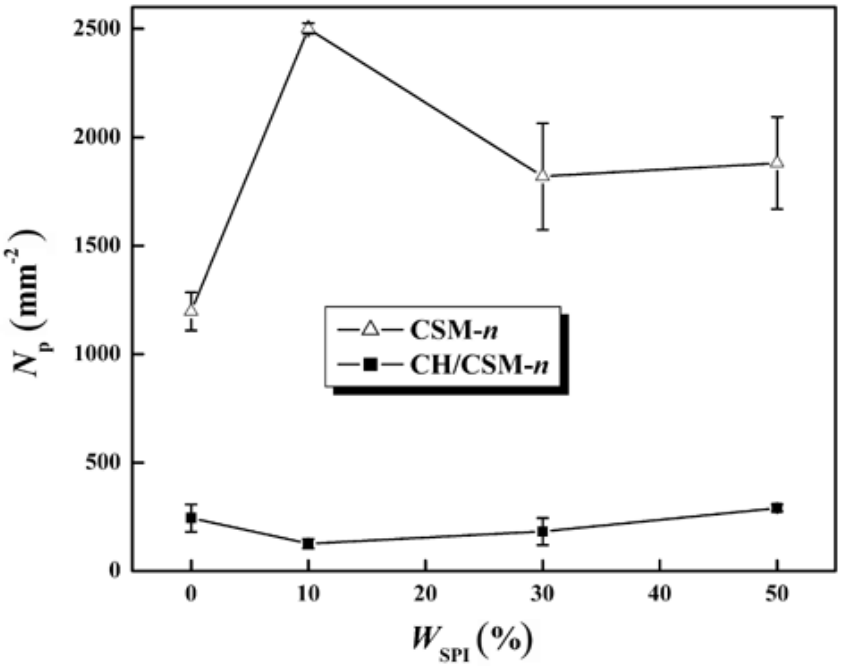

Fig. 10. Numbers of platelets (N_p) adhered to CSM-*n* and CH/CSM-*n* (*n* = 0, 10, 30, and 50) after 1 h of incubating platelets with the membranes

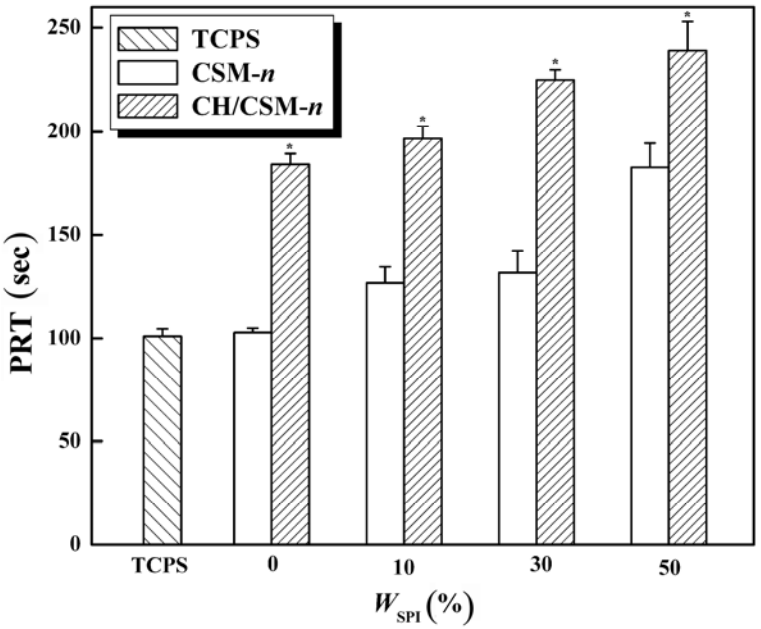

Fig. 11. Plasma recalcification time (PRT) for CSM-*n* and CH/CSM-*n* (*n* = 0, 10, 30, and 50). *P < 0.05 (CSM-*n* compared to CH/CSM-*n*)

Table 2. Hemolysis Rates (*HR*) of CSM-*n* and CH/CSM-*n* (*n* = 0, 10, 30, and 50) (N = 3, mean ± SD)

Samples	Optical density at 545 nm	*HR* (%)
Normal saline (Negative control)	0.031 ± 0.0002	0
Distilled water (Positive control)	0.68 ± 0.0220	100
CSM-0	0.04 ± 0.0023	1.56
CSM-10	0.04 ± 0.0028	1.57
CSM-30	0.066 ± 0.0037	5.46
CSM-50	0.10 ± 0.0220	10.81
CH/CSM-0	0.042 ± 0.0034	1.67
CH/CSM-10	0.042 ± 0.0041	1.69
CH/CSM-30	0.049 ± 0.0056	2.84
CH/CSM-50	0.05 ± 0.0032	2.89

CONCLUSIONS

1. Surface coating with chitosan was used to improve the physical properties and hemocompatibility of cellulose/SPI membranes (CSM-*n*).
2. The results of FTIR, XRD, and SEM observation confirmed that chitosan had coated and adhered to the original porous surface of the CSM-*n*, and ultimately formed a smooth surface. This resulted in an increase in mechanical properties, especially under wet conditions.
3. Cell culture experiments showed that L929 cells adhered to and grew well on the surface of the membranes. More cells attached to the surface of the chitosan-coated membranes (CH/CSM-*n*) than to the original CSM-*n*, indicating that surface coating with chitosan promoted the adherence and growth of L929 cells. Chitosan-coating altered the composition and microstructure of CSM-*n*, and slowed the dissolution of SPI into culture medium during cell culture, promoting cell proliferation and growth.
4. Hemocompatibility evaluations showed that a chitosan coating effectively decreased platelet adhesion, prolonged plasma recalcification time, and reduced hemolysis on the membrane surface. This work showed that surface coating with chitosan is a simple and effective way to improve mechanical properties, cytocompatibility, and hemocompatibility of cellulose/SPI membranes.

ACKNOWLEDGMENTS

This work was supported in part by the Natural Science Foundation for Distinguished Youth of Hubei Province (2007ABB025), the National Basic Research Program of China (973 Program, 2010CB732203), the Fundamental Research Funds for the Central Universities (6107003) and the Open Research Fund Program of Hubei-MOST KLOS & KLOBME (2009-1).

REFERENCES CITED

Abe, Y., and Mochizuki, A. (2003). "Hemodialysis membrane prepared from cellulose/n-methylmorpholine-n-oxide solution. III. The relationship between the drying condition of the membrane and its permeation behavior," *J. Appl. Polym. Sci.* 89(6), 1671-1681.

Almeida, E. V. R., Frollini, E., Castellan, A., and Coma, V. (2010). "Chitosan, sisal cellulose, and biocomposite chitosan/sisal cellulose films prepared from thiourea/NaOH aqueous solution," *Carbohydr. Polym.* 80(3), 655-664.

Bryjak, J., Aniulyte, J., and Liesiene, J. (2007). "Evaluation of man-tailored cellulose-based carriers in glucoamylase immobilization," *Carbohydr. Res.* 342(8), 1105-1109.

Cai, J., Zhang, L., Liu, S., Liu, Y., Xu, X., Chen, X., Chu, B., Guo, X., Xu, J., Cheng, H., Han, C. C., and Kuga, S. (2008). "Dynamic self-assembly induced rapid dissolution of cellulose at low temperatures," *Macromolecules* 41(23), 9345-9351.

Cai, J., Zhang, L., Zhou, J., Qi, H., Chen, H., Kondo, T., Chen, X., and Chu, B. (2007). "Multifilament fibers based on dissolution of cellulose in NaOH/urea aqueous solution: structure and properties," *Adv. Mater.* 19(6), 821-825.

Cai, K. Y., Yao, K. D., Cui, Y. L., Lin, S. B., Yang, Z. M., Li, X. Q., Xie, H. Q., Qing, T. W., and Luo, J. (2002). "Surface modification of poly (D, L-lactic acid) with chitosan and its effects on the culture of osteoblasts in vitro," *J. Biomed. Mater. Res.* 60(3), 398-404.

Chen, Y., and Zhang, L. (2004). "Blend membranes prepared from cellulose and soy protein isolate in NaOH/thiourea aqueous solution," *J. Appl. Polym. Sci.* 94(2), 748-757.

Chen, Y., Zhang, L., Gu, J., and Liu, J. (2004). "Physical properties of microporous membranes prepared by hydrolyzing cellulose/soy protein blends," *J. Membr. Sci.* 241(2), 393-402.

Cui, Y. L., Qi, A. D., Liu, W. G., Wang, X. H., Wang, H., Ma, D. M., and Yao, K. D. (2003). "Biomimetic surface modification of poly(l-lactic acid) with chitosan and its effects on articular chondrocytes in vitro," *Biomaterials* 24(21), 3859-3868.

Da Róz, A. L., Leite, F. L., Pereiro, L. V., Nascente, P. A. P., Zucolotto, V., Oliveira, Jr. O. N., and Carvalho, A. J. F. (2010). "Adsorption of chitosan on spin-coated cellulose films," *Carbohydr. Polym.* 80(1), 65-70.

Eller, L. K., and Reimer, R. A. (2010). "A high calcium, skim milk powder diet results in a lower fat mass in male, energy-restricted, obese rats more than a low calcium, casein, or soy protein diet," *J. Nutr.* 140(7), 1234-1241.

Entcheva, E., Bien, H., Yin, L., Chung, C. Y., Farrell, M., and Kostov, Y. (2004). "Functional cardiac cell constructs on cellulose-based scaffolding," *Biomaterials* 25(26), 5753-5762.

Franěk, F., Hohenwarter, O., and Katinger H. (2000). "Plant protein hydrolysates: Preparation of defined peptide fractions promoting growth and production in animal cells cultures," *Biotechnol. Prog.* 16(5) 688-692.

Giavaresi, G., Fini, M., Salvage, J., Aldini, N. N., Giardino, R., Ambrosio, L., Nicolais, L., and Santin, M. (2010). "Bone regeneration potential of a soybean-based filler: Experimental study in a rabbit cancellous bone defects," *J. Mater. Sci. Mater. Med.* 21(2), 615-626.

Guo, Z., Meng, S., Zhong, W., Du, Q. G., and Chou, L. S. L. (2009). "Self-assembly of silanated poly(ethylene glycol) on silicon and glass surfaces for improved haemocompatibility," *Appl. Surf. Sci.* 255(15), 6771-6780.

ISO 10993-4 (1999). "Biological evaluation of medical devices Part 4: Selection of tests for interactions with blood."

ISO 10993-5 (1999). "Biological evaluation of medical devices Part 5: Tests for in vitro cytotoxicity."

Kang, I. K., Kwon, O. H., Lee, Y. M., and Sung, Y. K. (1996). "Preparation and surface characterization of functional group-grafted and heparin-immobilized polyurethanes by plasma glow discharge," *Biomaterials* 17(8), 841-847.

Klemm, D., Heublein, B., Fink, H. P., and Bohn, A. (2005). "Cellulose: Fascinating biopolymer and sustainable raw material," *Angew. Chem. Int. Ed.* 44(22), 3358-3393.

Kumar, M. N. V. R. (2000). "A review of chitin and chitosan applications," *React. Funct. Polym.* 46(1), 1-27.

Kumar, R., Liu, D., and Zhang, L. (2008). "Advances in proteinous biomaterials," *J. Biobased Mater. Bio.* 2(1), 1-24.

Lee, Y. K., Kim, S. Y., Kim, K. H., Chun, B. H., Lee, K. H., Oh, D. J., and Chung, N. (2008). "Use of soybean protein hydrolysates for promoting proliferation of human keratinocytes in serum-free medium," *Biotechnol. Lett.* 30(11), 1931-1936.

Lin, C. H., Jao, W. C., Yeh, Y. H., Lin, W. C., and Yang, M. C. (2009). "Hemocompatibility and cytocompatibility of styrenesulfonate-grafted PDMS–polyurethane–HEMA hydrogel," *Colloids Surf., B.* 70(1), 132-141.

Liu, L., Guo, S. R., Chang, J., Ning, C. Q., Dong, C. M., and Yan, D. Y. (2008). "Surface modification of polycaprolactone membrane via layer-by-layer deposition for promoting blood compatibility," *J. Biomed. Mater. Res., Part B* 87(1), 244-250.

Lü, X. Y., Cui, W., Huang, Y., Zhao, Y., and Wang, Z. G. (2009). "Surface modification on silicon with chitosan and biological research," *Biomed. Mater.* 4(4), 044103.

Luo, L. H., Wang, X. M., Zhang, Y. F., Liu, Y. M., Chang, P. R., Wang, Y., and Chen Y. (2008). "Physical properties and biocompatibility of cellulose/soy protein isolate membranes coagulated from acetic aqueous solution," *J. Biomater. Sci. Polym. Ed.* 19(4), 479-496.

Luo, L. H., Zhang, Y. F., Wang, X. M., Wan, Y., Chang, P. R., Anderson, D. P., and Chen, Y. (2010). "Preparation, characterization, and in vitro and in vivo evaluation of cellulose/soy protein isolate composite sponges," *J. Biomater. Appl*. 24(6), 503-526.

Luo, X.G., and Zhang, L. (2010). "New solvents and functional materials prepared from cellulose solutions in alkali/urea aqueous system," *Food Res. Int.* in press. (doi:10.1016/j.foodres.2010.05.016.)

Merolli, A., Nicolais, L., Ambrosio, L., and Santin, M. (2010). "A degradable soybean-based biomaterial used effectively as a bone filler in vivo in a rabbit," *Biomed. Mater.* 5(1), 015008.

Müller, F. A., Müller, L., Hofmann, I., Greil, P., Wenzel, M. M., and Staudenmaier, R. (2006). "Cellulose-based scaffold materials for cartilage tissue engineering," *Biomaterials* 27(21), 3955-3963.

Murakami, R., and Takashima, R. (2003). "Mechanical properties of the capsules of chitosan–soy globulin polyelectrolyte complex," *Food Hydrocolloid.* 17(6), 885-888.

Pawlak, A., and Mucha, M. (2003). "Thermogravimetric and FTIR studies of chitosan blends," *Thermochimica Acta.* 396(1-2), 153-156.

Qi, G. Y., and Sun, X. S. (2010). "Peel adhesion properties of modified soy protein adhesive on a glass panel," *Ind. Crop. Prod.* 32(3), 208-212.

Qu, X. H., Wu, Q., and Chen, G. Q. (2006). "In vitro study on hemocompatibility and cytocompatibility of poly(3-hydroxybutyrate-co-3-hydroxyhexanoate)," *J. Biomater. Sci., Polym. Ed.* 17(10), 1107-1121.

Roy, R. K., Choi, H. W., Yi, J. W., Moon, M. W., Lee, K. R., Han, D. K., Shin, J. H., Kamijo, A., and Hasebe, T. (2009). "Hemocompatibility of surface-modified, silicon-incorporated, diamond-like carbon films," *Acta Biomater.* 5(1), 249-256.

Schurz, J. (1999). "'Trends in polymer science - A bright future for cellulose," *Prog. Polym. Sci.* 24(4), 481-483.

Serrano, M. C., Pagani, R., Vallet-Regí, M., Peña, J., Rámila, A., Izquierdo, I., and Portolés, M. T. (2004). "In vitro biocompatibility assessment of poly(e-caprolactone) films using L929 mouse fibroblasts," *Biomaterials* 25(25), 5603-5611.

Sharma, J. B., Gupta, N., and Mital, S. (2007). "Creation of neovagina using oxidized cellulose (surgicel) as a surgical treatment of vaginal agenesis," *Arch. Gynecol. Obstet*. 275(4), 231-235.

Shen, F., Zhang, E. L., and Wei, Z. J. (2010). "In vitro blood compatibility of poly (hydroxybutyrate-co-hydroxyhexanoate) and the influence of surface modification by alkali treatment," *Mater. Sci. Eng. C.* 30(3), 369-375.

Silva, S. S., Santos, M. I., Coutinho, O. P., Mano, J. F., and Reis, R. L. (2005). "Physical properties and biocompatibility of chitosan/soy blended membranes," *J. Mater. Sci.: Mater. Med.* 16(6), 575-579.

Suzuki, S., Grøndahl, L., Leavesley, D., Wentrup-Byrne, E. (2005). "In vitro bioactivity of MOEP grafted ePTFE membranes for craniofacial applications," *Biomaterials* 26(26), 5303-5312.

Uyama, Y., Kato, K., and Ikada, Y. (1998). "Surface modification of polymers by grafting," *Adv. Polym. Sci.* 137, 1-39.

Vaz, C. M., van Doeveren, P. F., Reis, R. L., and Cunha, A. M. (2003). "Soy matrix drug delivery systems obtained by melt-processing techniques," *Biomacromolecules* 4(6), 1520-1529.

Wang, L. C., Chen, X. G., Zhong, D. Y., and Xu, Q. C. (2007). "Study on poly(vinyl alcohol)/carboxymethyl-chitosan blend film as local drug delivery system," *J. Mater. Sci.: Mater. Med.* 18(6), 1125-1133.

Wen, X. W., Pei, S. P., Li, H., Ai, F., Chen, H., Li, K. Y., Wang, Q., and Zhang, Y. M. (2010). "Study on an antifouling and blood compatible poly(ethylene-vinyl acetate) material with fluorinated surface structure," *J. Mater. Sci.* 45(10), 2788-2797.

Xiao, Y. M., Li, D. X., Chen, X. N., Lu, J., Fan, H. S., and Zhang, X. D. (2008). "Preparation and cytocompatibility of chitosan-modified polylactide," *J. Appl. Polym. Sci.* 110(1), 408-412.

Zhang, W. F., Zhou, H. Y., Chen, X. G., Tang, S. H., and Zhang, J. J. (2009). "Biocompatibility study of theophylline/chitosan/*b*-cyclodextrin microspheres as pulmonary delivery carriers," *J. Mater. Sci.: Mater. Med.* 20(6), 1321-1330.

Zhao, J., Shi, Q. A., Yin, L. G., Luan, S. F., Shi, H. C., Song, L. J., Yin, J. H., and Stagnaro, P. (2010). "Polypropylene modified with 2-hydroxyethyl acrylate-g-2-methacryloyloxyethyl phosphorycholine and its hemocompatibility," *Appl. Surf. Sci.* 256(23), 7071-7076.

Article submitted: January 14, 2011; Peer review completed: February 16, 2011; Revised version received and accepted: March 9, 2011; Published: March 10, 2011.